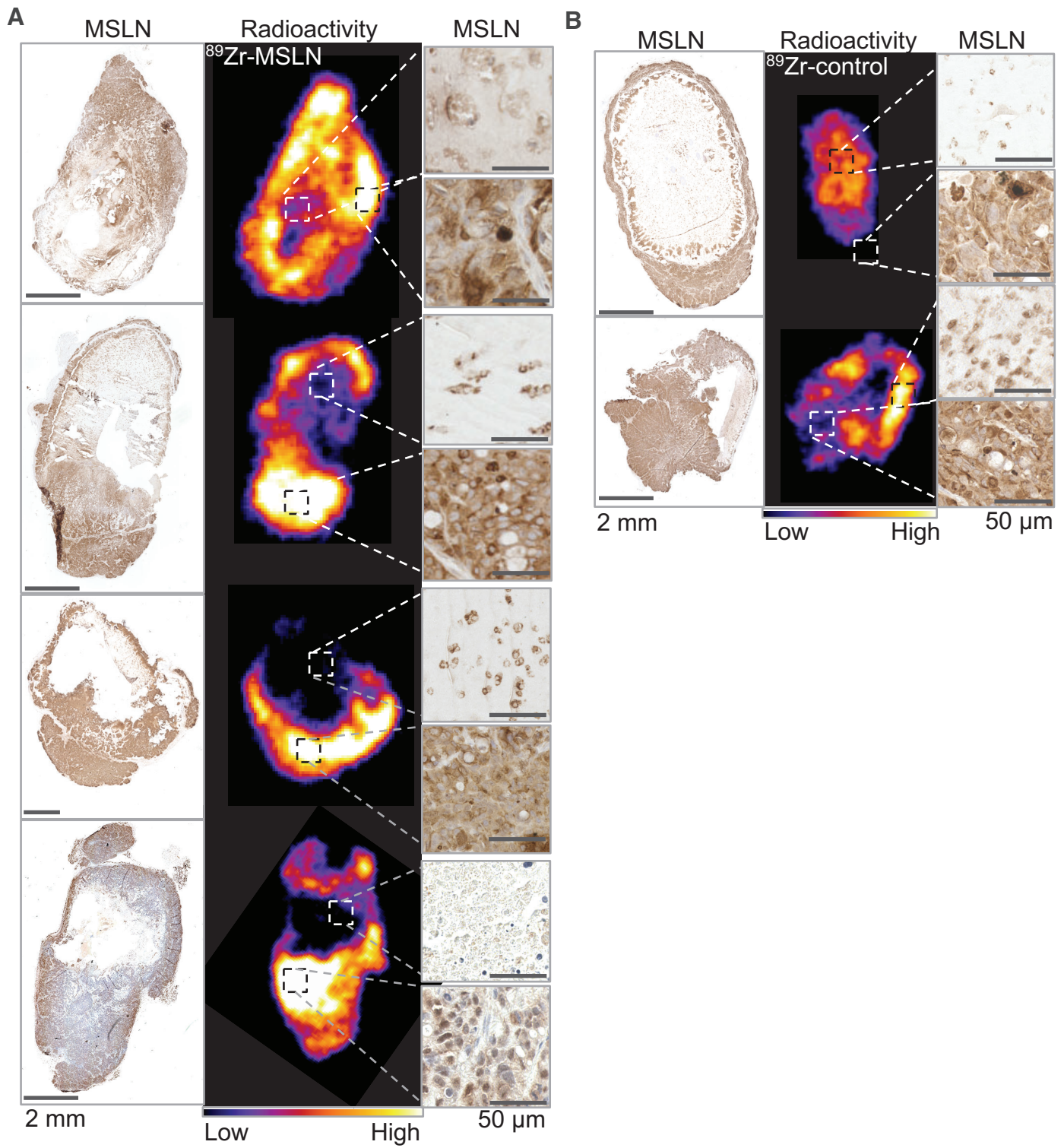


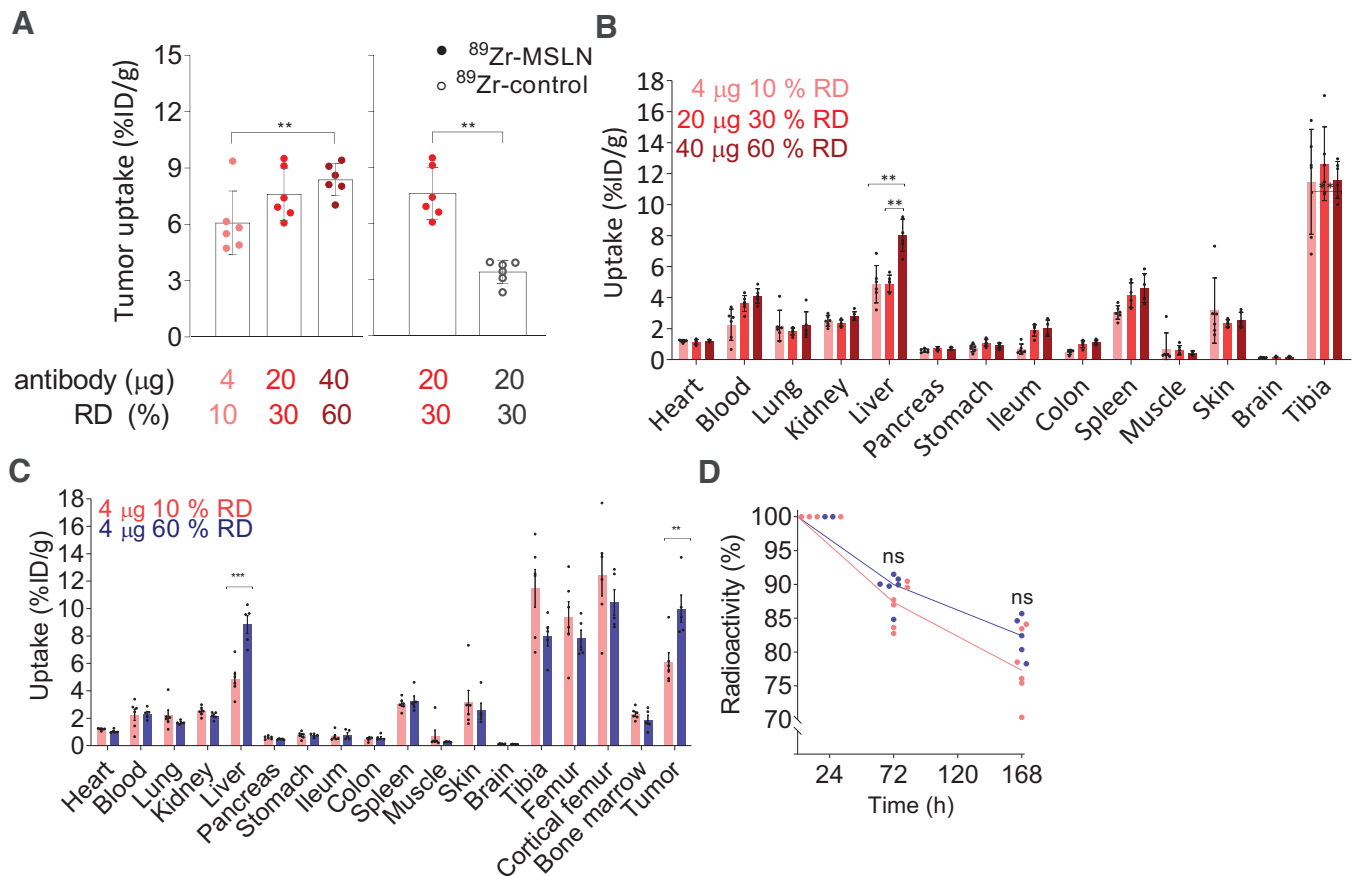
Supplemental Figure 1. ^{89}Zr -MSLN quality control

Ultra-performance liquid chromatography data of **A** optimized ^{89}Zr -MSLN, $4\% \pm 1\%$ antibody dimers and $15\% \pm 2\%$ radiolabeled dimers ($n = 6$) **B** immunoreactive fraction: 0.8 **C** $20 \mu\text{g}$ ^{89}Zr -MSLN preparation with 30% radioactive dimers **D** ^{89}Zr -MSLN with 10% vs 60% radioactive dimers (at 280 nm $\leq 5\%$ data not shown). On y-axis arbitrary units at 280 nm and millivolts at radioactivity detection. **E** *Ex vivo* tracer integrity of ^{89}Zr -MSLN in plasma 168 h pi ($n = 4$), determined by SDS PAGE, detected by autoradiography, R is ^{89}Zr -MSLN 7 days at RT, including free ^{89}Zr . LMW: low molecular weight. R: reference RAD: radioactivity detection Rh: recombinant human.



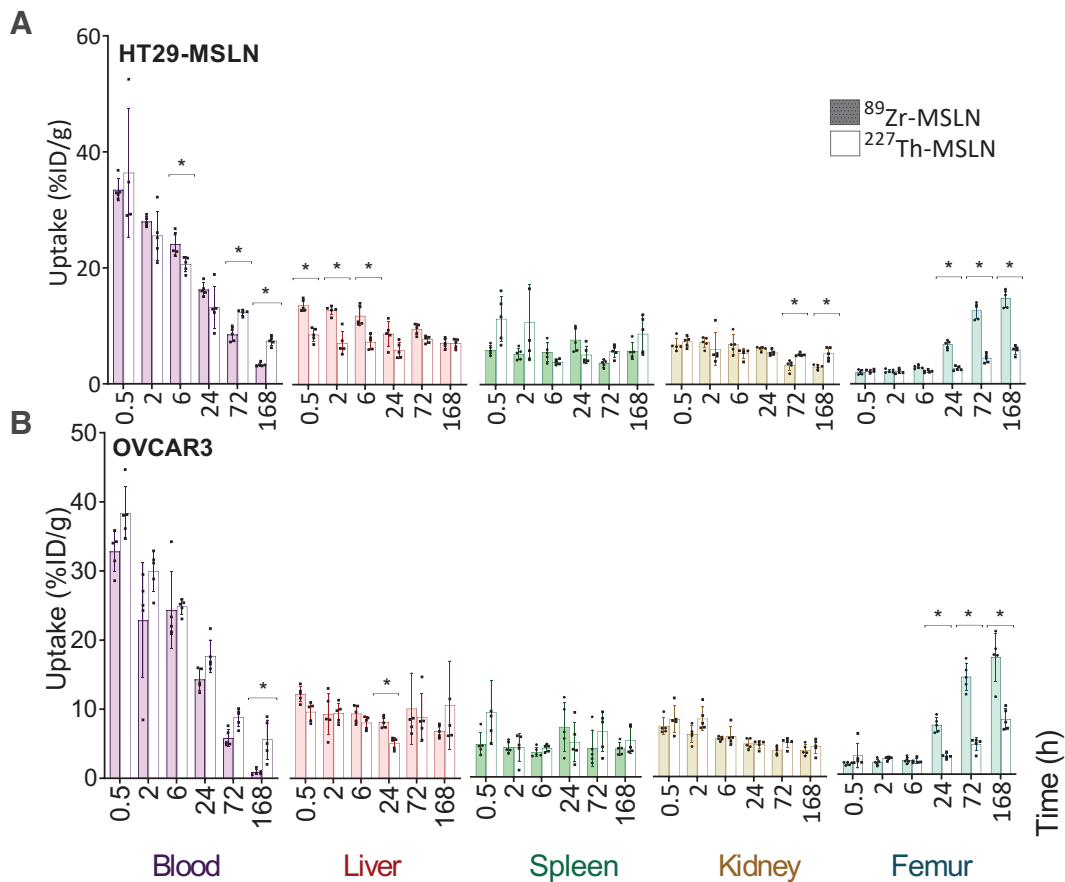
Supplemental Figure 2. Intratumoral $^{89}\text{Zr-MSLN}$ distribution

Mesothelin immunohistochemistry and autoradiography of HT29-MSLN formalin-fixed, paraffin-embedded tumor sections, that received **A** $^{89}\text{Zr-MSLN}$ or **B** $^{89}\text{Zr-control}$. Mesothelin immunohistochemistry and autoradiography are performed on the same tumor section. Radioactivity is simultaneously scaled in A and B from high to low ^{89}Zr signal intensity. MSLN, Mesothelin.



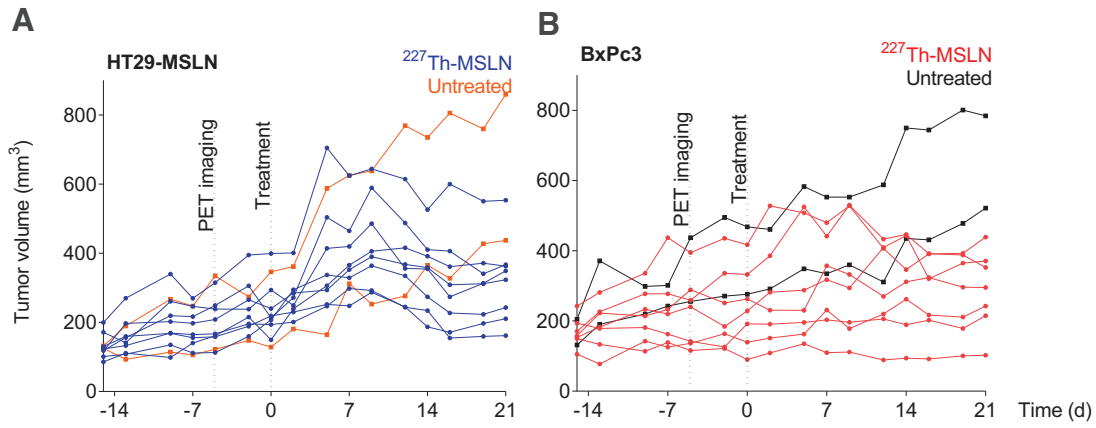
Supplemental Figure 3. Dose- and dimer-effect of ^{89}Zr -MSLN on tumor and healthy tissue uptake

In BxPc3 tumor-bearing mice at 168 h pi **A** *Ex vivo* tumor uptake of 4 μg 10% RD, 20 μg 30% RD, 40 μg 60% RD ^{89}Zr -MSLN and 20 μg 30% ^{89}Zr -control. **B** *Ex vivo* biodistribution of 4 μg 10% RD, 20 μg 30% RD and 40 μg 60% RD ^{89}Zr -MSLN. **C** *Ex vivo* biodistribution of 4 μg ^{89}Zr -MSLN and **D** *in vivo* tracer kinetics, expressed as radioactivity, corrected for decay, with 10% and 60% radioactive dimers. Uptake in tumor and healthy tissues is presented as percentage of injected dose per gram tissue (%ID/g), shown as mean \pm SD, including single data points. ***: $P < 0.001$ **: $P < 0.01$, with Bonferroni correction when comparing doses (A). RD: radioactive dimers.

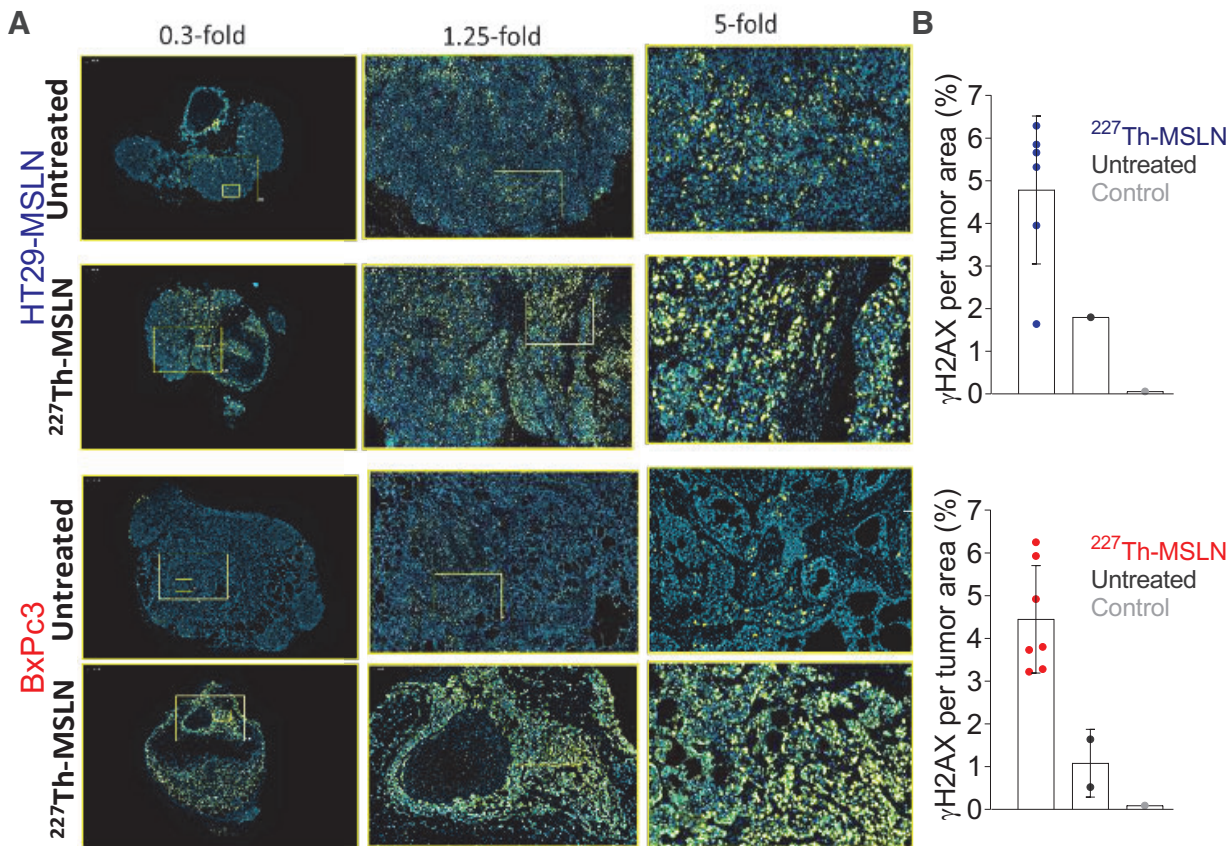


Supplemental Figure 4. *Ex vivo* biodistribution ⁸⁹Zr-MSLN vs ²²⁷Th-MSLN

in **A** HT29-MSLN tumor-bearing mice and **B** OVCAR3 tumor-bearing mice. Blood levels and uptake in kidney, liver, spleen and intact femur of 20 μg ⁸⁹Zr-MSLN (0.20 MBq) vs 20 μg ²²⁷Th-MSLN (0.015 MBq) at 0.5, 2, 6, 24, 72, and 168 h. Data is presented as mean percentage injected dose per gram tissue (%ID/g) \pm SD, including single data points. *: $P < 0.05$ with Bonferroni correction.



Supplemental Figure 5. Absolute tumor growth after ²²⁷Th-MSLN treatment of **A** HT29-MSLN tumor-bearing mice (n = 8) and **B** BxPc3 tumor-bearing mice (n = 7) treated with 0.75 mg/kg 500 kBq/kg ²²⁷Th-MSLN and n = 2 untreated mice per model. Tumor volumes expressed as mm³.



Supplemental Figure 6. γ H2AX expression in tumors of mice treated with ^{227}Th -MSLN

A γ H2AX immunofluorescence, marking double-strand DNA breaks, in HT29-MSLN and BxPc3 tumors of 0.75 mg/kg 500 kBq/kg ^{227}Th -MSLN treated (n = 6-7 per group) and untreated mice (n = 1-2 per group) harvested 21 days after injection **B** and quantification expressed as % γ H2AX per tumor area. Data are mean \pm SD, including single data points. Control: monoclonal mouse IgG2a antibody staining control. γ H2AX: gamma H2A histone family member X.

γ H2AX immunofluorescence

DNA double-strand breaks were detected with immunofluorescence using a human-specific gamma H2A histone family member X (γ H2AX) antibody (Cell Signaling, Clone JBW301, mouse), and a monoclonal mouse IgG2a antibody, clone DAK-GO5 (DAKO) was used as control (dilution 1:2000). Sections were exposed to a Cy3-labeled anti-murine-reactive antibody (Perkin Elmer; Opal™ 4-Color Fluorescent IHC Kit). Tumor sections were counter-stained using DAPI. γ H2AX foci were quantified using the HS Analysis Webkit tool (HS Analysis; Karlsruhe Institute of Technology, Germany).

Supplemental Table 1: ⁸⁹Zr-MSLN development for *in vivo* studies: critical conditions

Optimal conditions ⁸⁹Zr-MSLN production:	
Buffer exchange method	PD gravity filtration with HEPES 0.5 M pH 6.7
⁸⁹ Zr labeling conditions	0.1 mg/mL MSLN-3,2-HOPO concentration 250-500 MBq/mg specific activity In HEPES buffer
Purification method	PD10 gravity filtration purification, elution with: 10 mM histidine 130 mM glycine buffer pH 7.4
<u>Avoid the following conditions to limit radioactive dimer formation:</u>	
Buffer exchange method	Ultracentrifugation (Vivaspin) or NaCl 0.9%
⁸⁹ Zr labeling condition	> 0.1 mg/mL MSLN-HOPO concentration < 200 MBq/mg specific activity Buffers: <ul style="list-style-type: none">• Ammonium acetate pH 7• Ammonium acetate pH 5.5• Citrate buffer 30 mM• Addition of cold ⁸⁹Zr
Purification method	Purification by ultracentrifugation (Vivaspin) PD purification with: <ul style="list-style-type: none">• NaCl 0.9%• HEPES 0.5 M pH 7• EDTA addition before purification• Gentisic acid• Tris buffer pH 8.5• Sodium phosphate buffer pH 7• Sodium phosphate buffer pH 8.5• Histidine glycine 10/130 mM pH 8.5• Glucose 5%• Arginine glycine 50/50 mM pH 8.5

PD: protein desalting, EDTA: ethylenediamine tetraacetic acid.

Supplemental Table 2: ^{89}Zr -MSLN and ^{227}Th -MSLN batches for *in vivo* studies

	^{89}Zr -MSLN				^{89}Zr -control	^{227}Th -MSLN
Antibody dose (μg)	4	4	20	40	20	20
Radioactive dose (MBq)	1	1	3	3	4	0.015
Radiolabeling efficiency (%)	60	60	64	92	76	99
Antibody concentration (mg/ml)	0.1	0.1	0.2	0.4	0.2	0.2
Specific activity (MBq/mg)	400	400	250	125	250	0.7
Radiochemical purity (%)	99	99	97	99	98	99
Radioactive dimers (%)	10	60	30	60	30	<10
Total antibody dimers (%)	<5	5	5	5	5	<5

Batches of 4 μg and 40 μg ^{89}Zr -MSLN were injected in the BxPc3 tumor-bearing mice (Suppl. Fig. 3), 20 μg ^{89}Zr -MSLN and ^{89}Zr -control were injected in HT29-MSLN tumor-bearing mice (Fig. 1). The 20 μg ^{227}Th -MSLN was injected in HT29-MSLN tumor-bearing mice (Fig. 5).